

Benzothiadiazole and Its Derivatives-based sp^2 Carbon-Conjugated Covalent Organic Frameworks for Photocatalytic Hydrogen Generation

Chao-Qin Han,[†] Xiaokang Sun,[†] Xiao Liang,[†] Lei Wang,^{*,†} Hanlin Hu,[†] Xiao-Yuan Liu,^{*,†}

[†] Hoffmann Institute of Advanced Materials, Shenzhen Polytechnic, 7098 Liuxian Blvd,
Nanshan District, Shenzhen, 518055, P.R. China

* To whom correspondence should be addressed: wliam@szpt.edu.cn and

liuxiaoyuan1989@szpt.edu.cn

Materials

Anisole, tetrabutylammonium hydroxide (TBAH, 25% in methanol), chloroplatinic acid (H_2PtCl_6), ascorbic acid (AA), triethanolamine (TEOA) and o-dichlorobenzene (o-DCB) were purchased from Shanghai Aladdin Biochemical Technology Co. Ltd. P-xylylenedicyanide (PDAN), 2,2'-([2,2'-bipyridine]-5,5'-diyl)diacetonitrile (BPyDAN), 4,7-dibromobenzo[c][1,2,5]selenadiazole and 4,9-dibromonaphtho[2,3-c][1,2,5]thiadiazole were purchased from Shanghai Bidepharm Co., Ltd. 5'-(4,4,5,5-tetramethyl-1,3,2-dioxaborolan-2-yl)-[1,1':3',1''-terphenyl]-4,4''-dicarbaldehyde was purchased from Jilin Chinese Academy of Science-Yanshen Technology Co., Ltd. 5',5'''-(benzo[c][1,2,5]thiadiazole-4,7-diyl)bis((1,1':3',1''-terphenyl)-4,4''-dicarbaldehyde) (BT-TDA) was synthesized according to the reported work. All commercially available reagents were used without further purification.

Characterization

Powder X-ray diffraction (PXRD) patterns for synthesized COFs were measured using Bruker D8Advance X-ray diffractometer with Cu $K\alpha$ radiation. The solid-state ^{13}C cross polarization magic angle spinning NMR spectra were measured on a Bruker AVANCE III 600 M. Fourier transform infrared (FT-IR) spectra were recorded from 500 to 4000 cm^{-1} on a PerkinElmer spectrometer. The Steady-state photoluminescent spectra were recorded on FLS1000 spectrofluorometer (Edinburgh Instruments). The UV-vis spectra were measured on Shimadzu UV-3600 spectrophotometer. Scanning electron micrographs (SEM) images were taken using a JEOLJSM-IT800(SHL). The thermogravimetric data was collected using TGA 550 analyzer and the samples were heated from room temperature to 800°C at a ramp rate of 10°C / min. Gas chromatographic (GC) analysis was carried out on a CEAULIGHT GC-7920 instrument

equipped with a thermal conductivity detector (TCD) using high pure nitrogen as the carrier gas. Small angle X-ray scattering (SAXS) at Shanghai Synchrotron Radiation Facility (Shanghai, China). The two-dimensional scattering data were collected by using a PILATUS 2 M (Dectris Ltd., Switzerland) detector with a pixel size of $172\ \mu\text{m} \times 172\ \mu\text{m}$, with the distance from the sample to the detector set to 1981 mm. An incident photon energy of 10 keV was applied, with a corresponding wavelength of 0.124 nm. To avoid detector saturation, two beam stops were placed before the detector to block the direct incident beam and reflected beam. One-dimensional experimental data were obtained with the SGTools software package programmed by Zhao et al¹. Transmission electron microscope (TEM) was performed by JEOLJEM 2100F. X-ray photoelectron spectroscopy (XPS) was carried out on a Thermo ESCALAB 250XI XPS spectrometer. Nitrogen sorption isotherms were collected by automated volumetric adsorption apparatus (Micromeritics, 3Flex). The Brunauer-Emmett-Teller (BET) method was utilized to calculate the specific surface area and the nonlocal density functional theory (NLDFT) method was applied for the estimation of pore size distribution. The electron paramagnetic resonance (EPR) measurements were performed by Bruker EMX-plus.

Photoelectrochemical Measurements

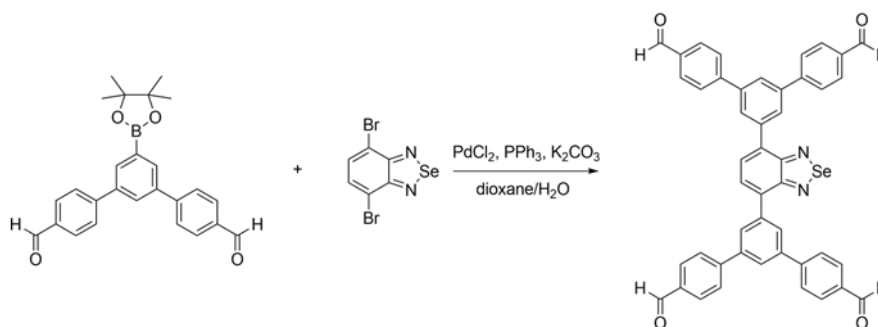
Photoelectrochemical measurements were conducted with a CHI660E (CH Instrument Corp, Shanghai) electrochemical workstation. Firstly, 5 mg of HIAM-000X ($X = 1, 2, 3, 4, 5, 6$) were added into a mixed solution of 1 mL of ethanol and 10 μL of 5 wt% Nafion, which was ultrasonicated for two hours to get homogeneous suspension. Then, HIAM-000X suspension was dropped on the surface of ITO glass and dried at room temperature. A standard three electrode system was used with the photocatalyst-coated ITO glass as the working electrode, Pt wire as

the counter electrode and an Ag/AgCl as a reference electrode. 0.1 M Na₂SO₄ aqueous solution was used as the electrolyte, and Mott-Schottky measurement was carried out at frequency of 1000-1500 Hz with amplitude of 5 mV.

Photocatalytic Hydrogen Evolution Test

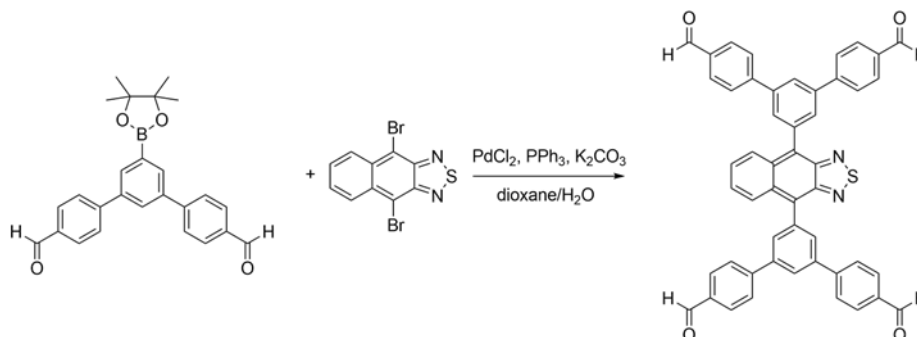
10 mg HIAM-000X (X = 1, 2, 3, 4, 5, 6) was well dispersed in 50 mL deionized water containing 25% vol triethanolamine (TEOA) as the sacrificial agent, 0.01 M chloroplatinic acid (H₂PtCl₆) aqueous solution (12 wt% Pt) was introduced into the reaction system. When 0.1 M ascorbic acid (AA) was the sacrificial agent, 0.01 M chloroplatinic acid (H₂PtCl₆) aqueous solution (5 wt% Pt) was adopted while keep the same conditions. The reaction solution was evacuated under vacuum to completely discharge air and maintained at 6 °C in the circulating cooling system. After that the reaction system was irradiated vertically under 300 W xenon lamp with $\lambda > 420$ nm cut-off filter. When TEOA or AA is used as sacrificial reagent, the average rate was obtained by photocatalysis for five hours including one hours of in-situ photo deposition. For long-term experiments, 10 mg HIAM-000X was adopted with 50 mL deionized water containing 25 vol% TEOA (12 wt% Pt) or 0.1 M AA (5 wt% Pt) and radiated under 300 W xenon lamp with $\lambda > 420$ nm cut-off filter, 1 h in situ photo deposition was used in all experiments.

Synthesis of 5',5''''-(benzo[c][1,2,5]selenadiazole-4,7-diyl)bis((1,1':3',1''-terphenyl)-4,4''-dicarbaldehyde) (BS-TDA)



4,7-dibromobenzo[c][1,2,5]selenadiazole (2.0 mmol, 0.68 g), 5'-(4,4,5,5-tetramethyl-1,3,2-dioxaborolan-2-yl)-[1,1':3',1''-terphenyl]-4,4''-dicarbaldehyde (4.4 mmol, 1.82 g), PdCl₂ (0.2 mmol, 35.0 mg), PPh₃ (0.4 mmol, 0.11 g) and K₂CO₃ (8.0 mmol, 1.10 g) were added into one 250 mL round-bottle flask containing 80 mL dioxane and 20 mL water. The mixture was degassed four times and stirred at 105°C for 6 hours. During the reaction, yellow precipitates gradually generated. After cooling down to room temperature, the precipitate was filtrated to offer 5',5''''-(benzo[c][1,2,5]selenadiazole-4,7-diyl)bis((1,1':3',1''-terphenyl)-4,4''-dicarbaldehyde) as a yellow solid (1.46 g, 97.2%).

Synthesis of 5',5''''-(naphtho[2,3-c][1,2,5]thiadiazole-4,9-diyl)bis((1,1':3',1''-terphenyl)-4,4''-dicarbaldehyde) (NT-TDA)



4,9-dibromonaphtho[2,3-c][1,2,5]thiadiazole (2.0 mmol, 0.69 g), 5'-(4,4,5,5-tetramethyl-1,3,2-dioxaborolan-2-yl)-[1,1':3',1''-terphenyl]-4,4''-dicarbaldehyde (4.4 mmol, 1.82 g), PdCl₂ (0.2

mmol, 35.0 mg), PPh₃ (0.4 mmol, 0.11 g) and K₂CO₃ (8.0 mmol, 1.10 g) were added into one 250 mL round-bottle flask containing 80 mL dioxane and 20 mL water. The mixture was degassed four times and stirred at 105°C for 6 hours. During the reaction, orange precipitates gradually generated. After cooling down to room temperature, the precipitate was filtrated to offer 5',5''-(naphtho[2,3-c][1,2,5]thiadiazole-4,9-diyl)bis((1,1':3',1''-terphenyl)-4,4''-dicarbaldehyde) as an orange solid (1.43 g, 94.8%).

Synthesis of sp²-COFs.

Synthesis of HIAM-0001.

HIAM-0001 was synthesized according to previous literature with a slight modification². A Pyrex tube (10 mL) containing BT-TDA (15 mg, 0.021 mmol), PDAN (7 mg, 0.042 mmol) and anisole/EtOH (1 mL, 1/1) was sonicated for 10 min. Then TBAH (25% in MeOH, 60 μL) solution was added to the above mixture solution. The tube was degassed through three freeze-pump-thaw cycles and then kept at 120 °C for 72 h. After cooling to room temperature, the precipitate was collected by filtration and washed with THF for several times., the yellow solid was Soxhlet extracted in THF for 24 h and dried under 60 °C vacuum to afford HIAM-0001.

Synthesis of HIAM-0002.

A Pyrex tube (10 mL) containing BS-TDA (15 mg, 0.021 mmol), PDAN (7 mg, 0.042 mmol) and anisole/EtOH (1 mL, 1/1) was sonicated for 10 min. Then TBAH (25% in MeOH, 40 μL) solution was added to the above mixture solution. The tube was degassed through three freeze-pump-thaw cycles and then kept at 150 °C for 72 h. After cooling to room temperature, the precipitate was collected by filtration and washed with THF for several times. The deep yellow

solid was Soxhlet extracted in THF for 24h and dried under 60 °C vacuum to afford HIAM-0002.

Synthesis of HIAM-0003.

A Pyrex tube (10 mL) containing NT-TDA (16 mg, 0.021 mmol), PDAN (13 mg, 0.084 mmol) and anisole/EtOH (1 mL, 1/1) was sonicated for 10 min. Then TBAH (25% in MeOH, 40 µL) solution was added to the above mixture solution. The tube was degassed through three freeze-pump-thaw cycles and then kept at 120 °C for 72 h. After cooling to room temperature, the precipitate was collected by filtration and washed with THF for several times. The red solid was Soxhlet extracted in THF for 24h and dried under 60 °C vacuum to afford HIAM-0003.

Synthesis of HIAM-0004.

HIAM-0004 was synthesized according to previous literature with a slight modification². A Pyrex tube (10 mL) containing BT-TDA (15 mg, 0.021 mmol), BPyDAN (10 mg, 0.042 mmol) and DCB/EtOH (1 mL, 1/1) was sonicated for 10 min. Then TBAH (25% in MeOH, 40 µL) solution was added to the above mixture solution. The tube was degassed through three freeze-pump-thaw cycles and then kept at 150 °C for 72 h. After cooling to room temperature, the precipitate was collected by filtration and washed with THF for several times. The yellow solid was Soxhlet extracted in THF for 24h and dried under 60 °C vacuum to afford HIAM-0004.

Synthesis of HIAM-0005.

A Pyrex tube (10 mL) containing BS-TDA (15 mg, 0.021 mmol), BPyDAN (10 mg, 0.042 mmol) and DCB/EtOH (1 mL, 1/1) was sonicated for 10 min. Then TBAH (25% in MeOH, 20 µL) solution was added to the above mixture solution. The tube was degassed through three freeze-pump-thaw cycles and then kept at 150 °C for 72 h. After cooling to room temperature,

the precipitate was collected by filtration and washed with THF for several times. The yellow solid was Soxhlet extracted in THF for 24h and dried under 60 °C vacuum to afford HIAM-0005.

Synthesis of HIAM-0006.

A Pyrex tube (10 mL) containing NT-TDA (16 mg, 0.021 mmol), BPyDAN (15 mg, 0.063 mmol) and DCB/EtOH (1 mL, 1/1) was sonicated for 10 min. Then TBAH (25% in MeOH, 60 µL) solution was added to the above mixture solution. The tube was degassed through three freeze-pump-thaw cycles with kept at 150 °C for 72 h. After cooling to room temperature, the precipitate was collected by filtration and washed with THF for several times. the dark red solid was Soxhlet extracted in THF for 24h and dried under 60 °C vacuum to afford HIAM-0006.

Table S1. Solvothermal conditions and corresponding results of crystallinity for HIAM-COFs.

The ratio of Monomer	Solvent (1mL,1/1)	Catalyst (TBAH)	Temperature	Time	Crystallinity
BT-TDA/PDAN(1:2)	Anisole/EtOH	40 μ L	120 $^{\circ}$ C	3d	None
	Anisole/EtOH	40 μ L	150 $^{\circ}$ C	3d	None
	Anisole/EtOH	60 μ L	120 $^{\circ}$ C	3d	Strong
BS-TDA/PDAN(1:2)	Anisole/EtOH	40 μ L	120 $^{\circ}$ C	3d	None
	Anisole/EtOH	60 μ L	120 $^{\circ}$ C	3d	None
	Anisole/EtOH	40 μ L	150 $^{\circ}$ C	3d	Strong
NS-TDA/PDAN(1:2)	Anisole/EtOH	40 μ L	120 $^{\circ}$ C	3d	None
	Anisole/EtOH	40 μ L	150 $^{\circ}$ C	3d	None
	Anisole/EtOH	60 μ L	150 $^{\circ}$ C	3d	None
	Anisole/EtOH	80 μ L	150 $^{\circ}$ C	3d	None
	Anisole/EtOH	100 μ L	150 $^{\circ}$ C	3d	None
NS-TDA/PDAN (1:3)	Anisole/EtOH	20 μ L	150 $^{\circ}$ C	3d	None
	Anisole/EtOH	40 μ L	150 $^{\circ}$ C	3d	None
	Anisole/EtOH	60 μ L	150 $^{\circ}$ C	3d	None
	Anisole/EtOH	80 μ L	150 $^{\circ}$ C	3d	None
NS-TDA/PDAN (1:4)	Anisole/EtOH	20 μ L	120 $^{\circ}$ C	3d	Weak
	Anisole/EtOH	20 μ L	150 $^{\circ}$ C	3d	Weak
	Anisole/EtOH	40 μ L	120 $^{\circ}$ C	3d	Strong
	Anisole/EtOH	40 μ L	150 $^{\circ}$ C	3d	Weak
	Anisole/EtOH	60 μ L	120 $^{\circ}$ C	3d	Weak
	Anisole/EtOH	60 μ L	120 $^{\circ}$ C	3d	Weak
BT-TDA/BPyDAN(1:2)	DCB/EtOH	20 μ L	120 $^{\circ}$ C	3d	Weak
	DCB/EtOH	30 μ L	120 $^{\circ}$ C	3d	None
	DCB/EtOH	40 μ L	120 $^{\circ}$ C	3d	None
	DCB/EtOH	60 μ L	120 $^{\circ}$ C	3d	None
	DCB/EtOH	20 μ L	150 $^{\circ}$ C	3d	None
	DCB/EtOH	40 μ L	150 $^{\circ}$ C	3d	Strong
	DCB/EtOH	60 μ L	150 $^{\circ}$ C	3d	None
BS-TDA/BPyDAN(1:2)	DCB/EtOH	20 μ L	120 $^{\circ}$ C	3d	None
	DCB/EtOH	40 μ L	120 $^{\circ}$ C	3d	None
	DCB/EtOH	60 μ L	120 $^{\circ}$ C	3d	None
	DCB/EtOH	20 μ L	150 $^{\circ}$ C	3d	Strong
	DCB/EtOH	40 μ L	150 $^{\circ}$ C	3d	None
	DCB/EtOH	60 μ L	150 $^{\circ}$ C	3d	None
NS-TDA/BPyDAN(1:2)	DCB/EtOH	20 μ L	150 $^{\circ}$ C	3d	None
	DCB/EtOH	40 μ L	150 $^{\circ}$ C	3d	None
	DCB/EtOH	60 μ L	150 $^{\circ}$ C	3d	None
NS-TDA/BPyDAN(1:3)	DCB/EtOH	20 μ L	150 $^{\circ}$ C	3d	Weak
	DCB/EtOH	40 μ L	150 $^{\circ}$ C	3d	Weak
	DCB/EtOH	60 μ L	150 $^{\circ}$ C	3d	Strong

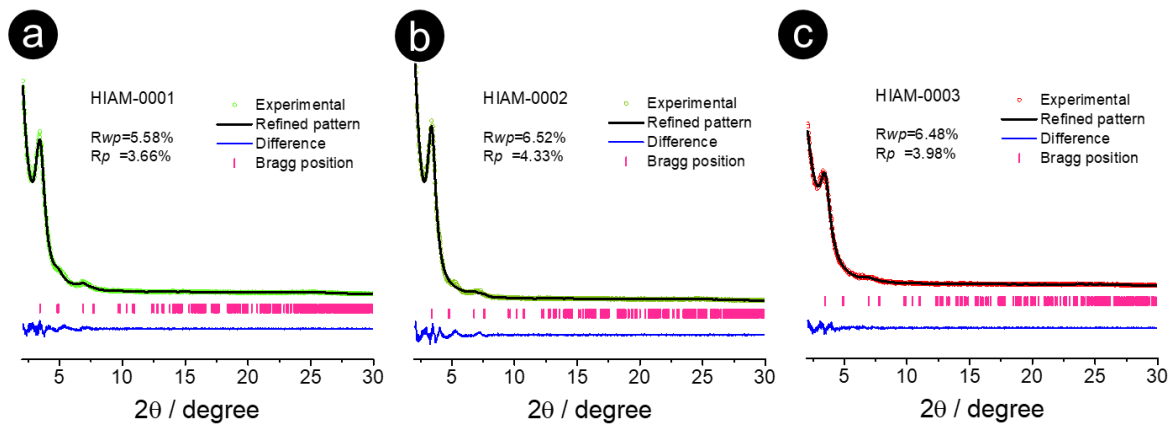


Fig. S1 The Pawley refinement PXRD Patterns of HIAM-0001 (a), HIAM-0002 (b), HIAM-0003 (c).

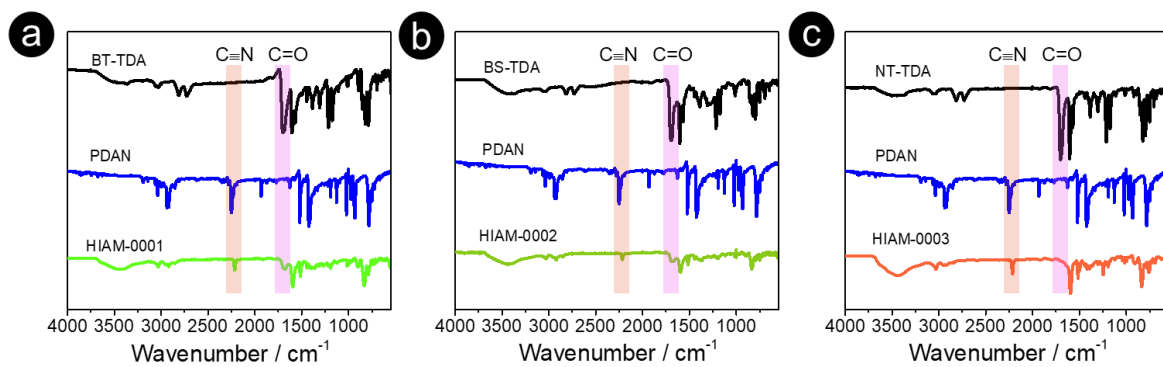


Fig. S2 FT-IR spectra of (a) HIAM-0001, (b) HIAM-0002 and (c) HIAM-0003.

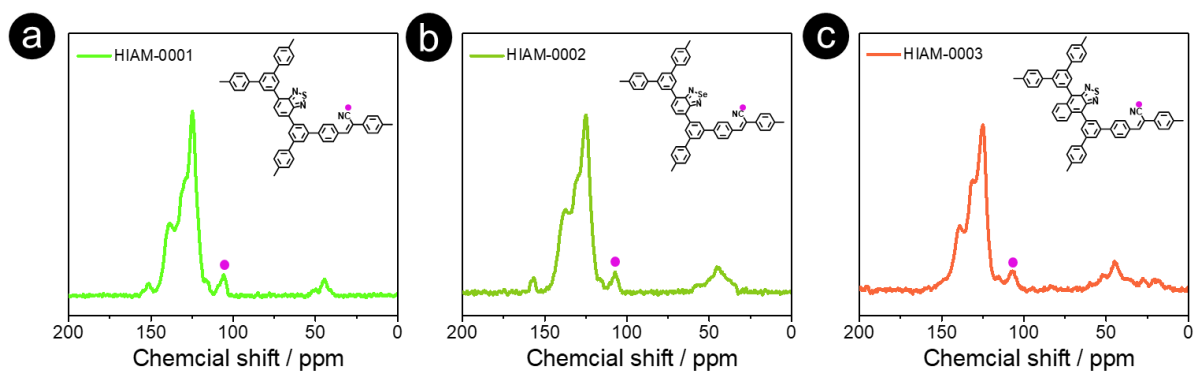


Fig. S3 Solid-state ^{13}C cross-polarization magic angle spinning NMR spectrum of (a) HIAM-0001, (b) HIAM-0002, (c) HIAM-0003.

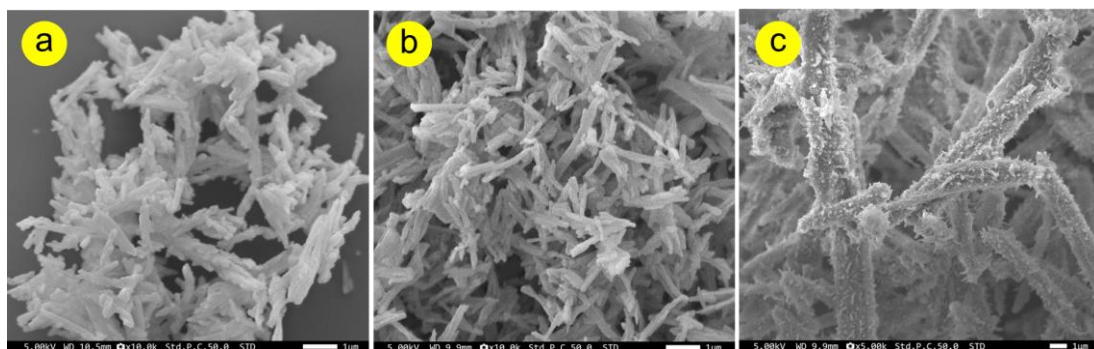


Fig. S4 SEM images of (a) HIAM-0001, (b) HIAM-0002 and (c) HIAM-0003.

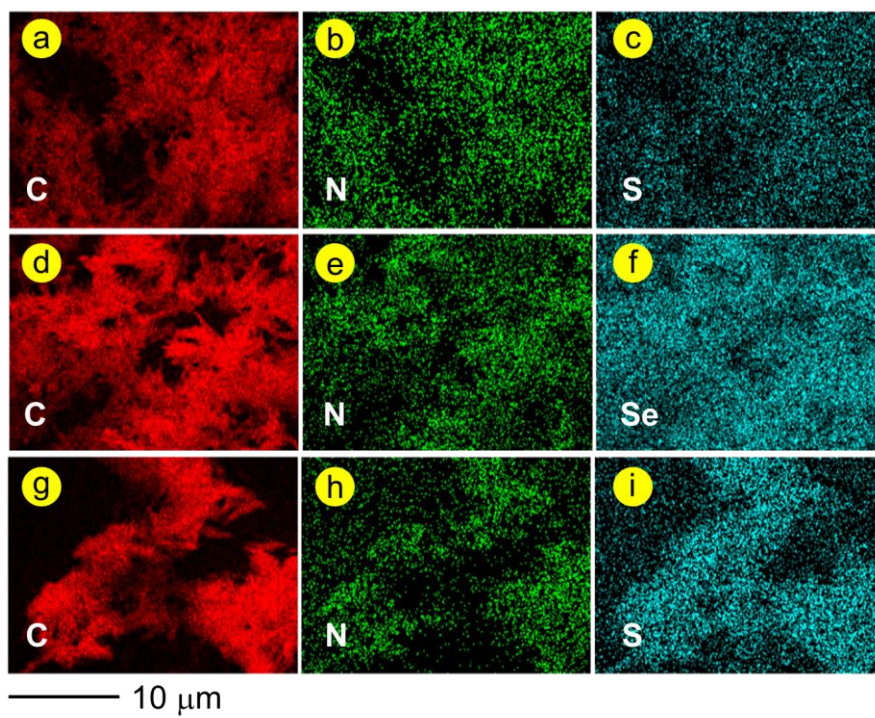


Fig. S5 Energy dispersive X-ray analysis of HIAM-0001 (a, b, c), HIAM-0002 (d, e, f) and HIAM-0003 (g, h, i).

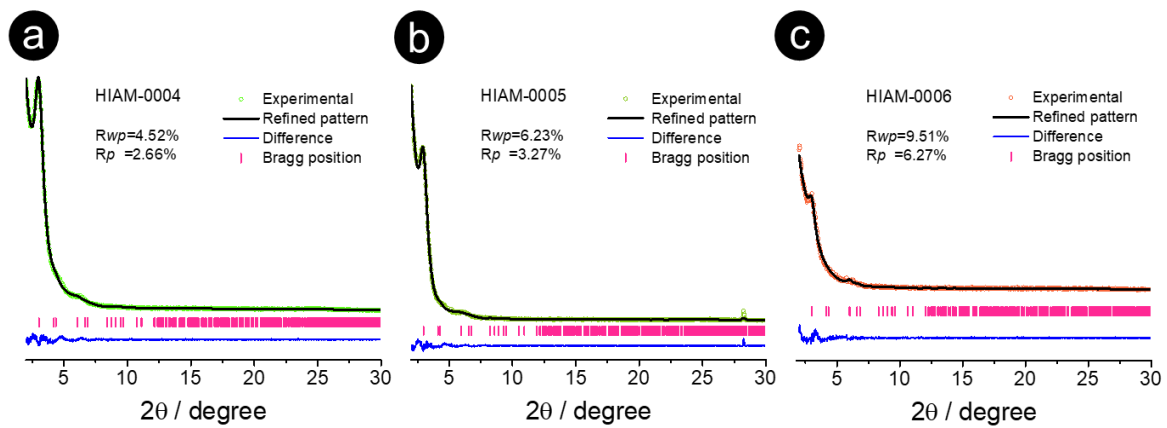


Fig. S6 The Pawley refinement PXRD Patterns of HIAM-0004 (a), HIAM-0005 (b), HIAM-0006 (c).

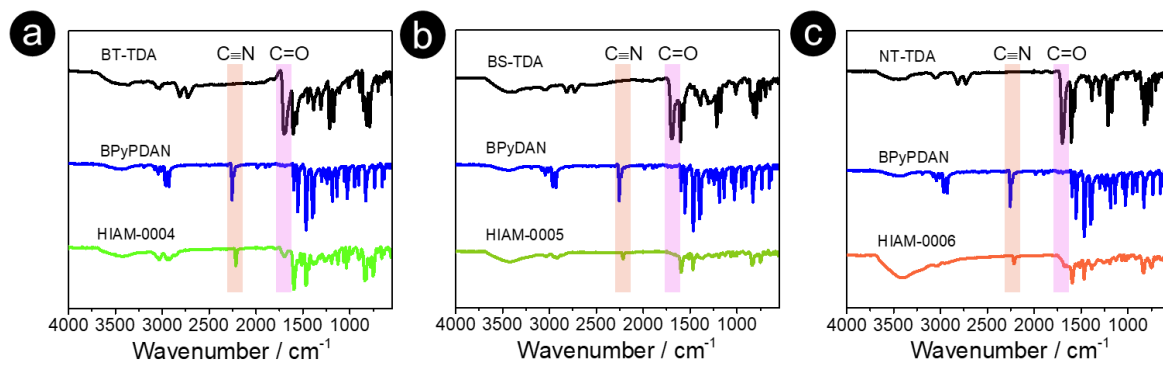


Fig. S7 FT-IR spectra of (a) HIAM-0004, (b) HIAM-0005 and (c) HIAM-0006.

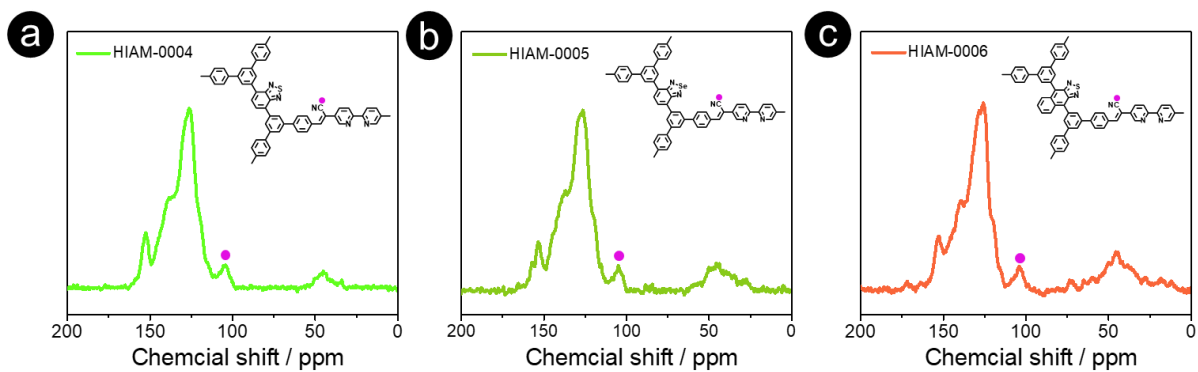


Fig. S8 Solid-state ^{13}C cross-polarization magic angle spinning NMR spectrum of (a) HIAM-0004, (b) HIAM-0005, (c) HIAM-0006.

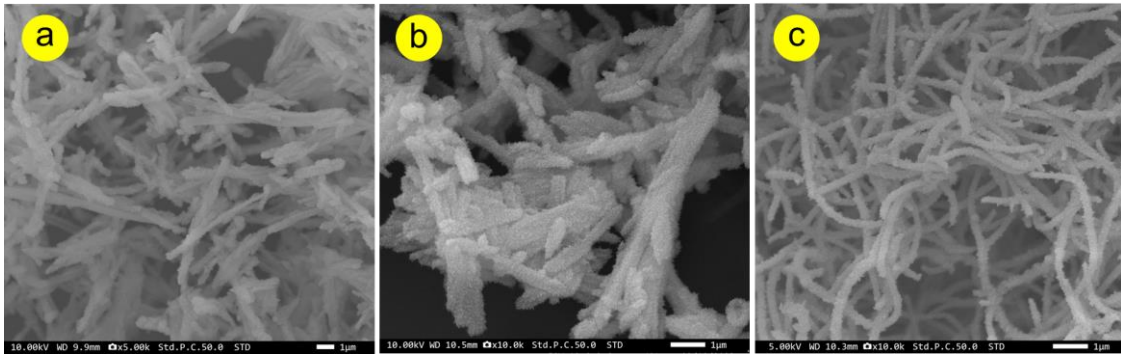


Fig. S9 SEM images of (a) HIAM-0004, (b) HIAM-0005 and (c) HIAM-0006.

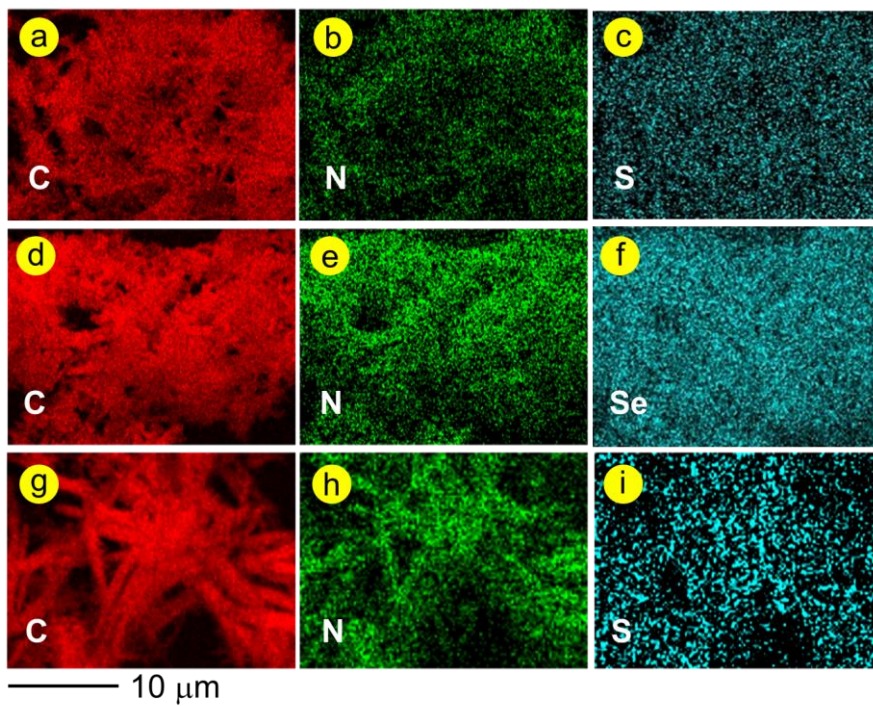


Fig. S10 Energy dispersive X-ray analysis of HIAM-0004 (a, b, c), HIAM-0005 (d, e, f) and HIAM-0006 (g, h, i).

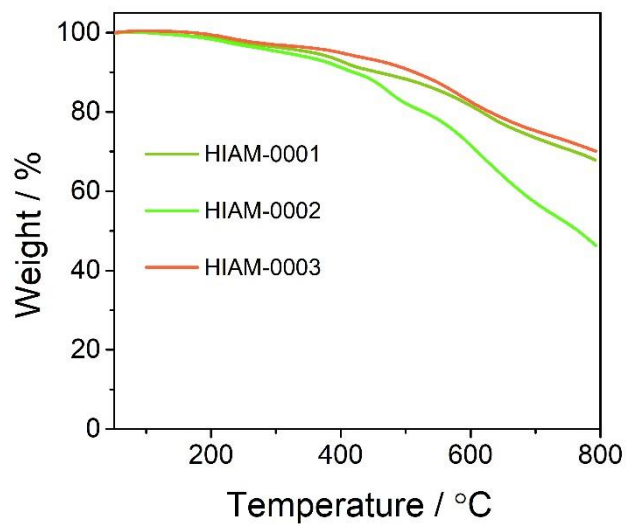


Fig. S11 TGA curves of HIAM-0001, HIAM-0002 and HIAM-0003.

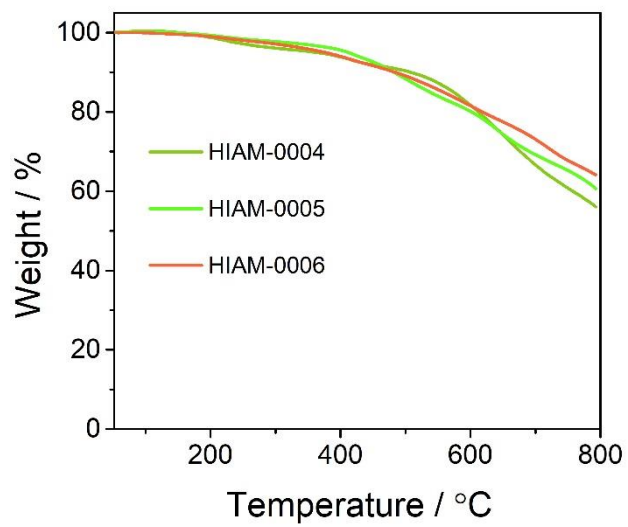


Fig. S12 TGA curves of HIAM-0004, HIAM-0005 and HIAM-0006.

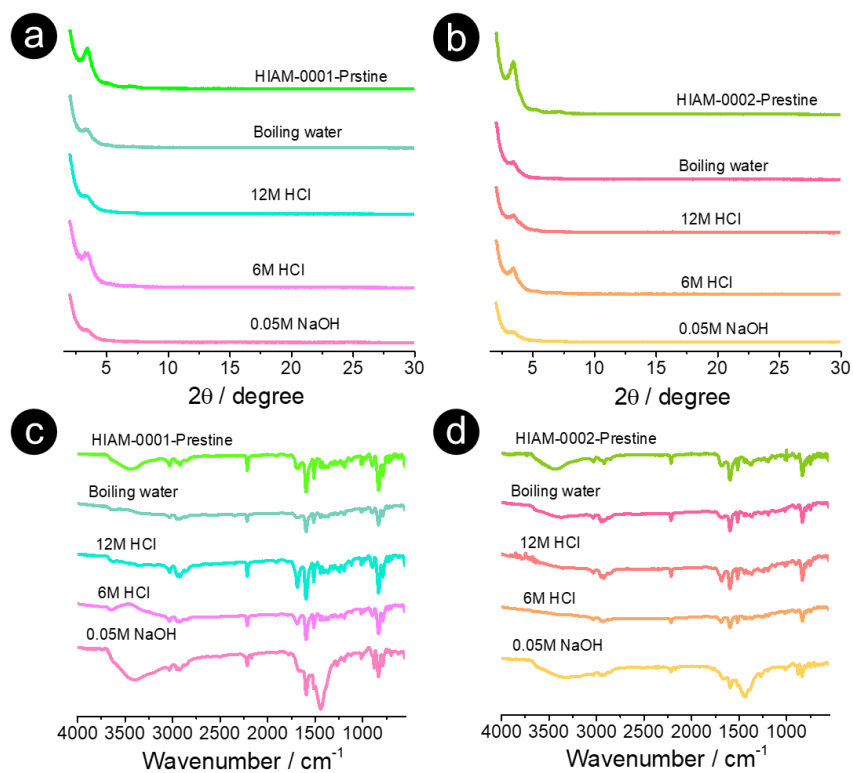


Fig. S13 (a, b) PXRD patterns and (c, d) FT-IR spectra for HIAM-0001 and HIAM-0002 after soaking in H_2O (100 $^\circ\text{C}$), HCl (12 M), HCl (6 M) and NaOH (0.05 M) for 24 hours.

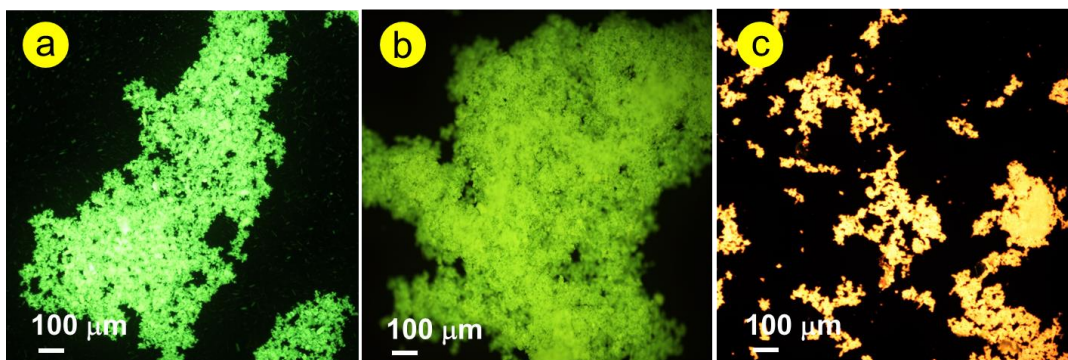


Fig. S14 Optical pictures of (a) HIAM-0001, (b) HIAM-0002 and (c) HIAM-0003.

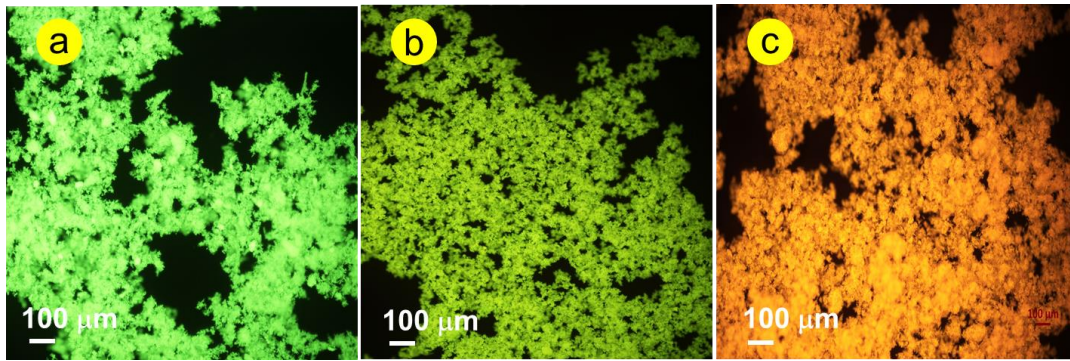


Fig. S15 Optical pictures of (a) HIAM-0004, (b) HIAM-0005 and (c) HIAM-0006.

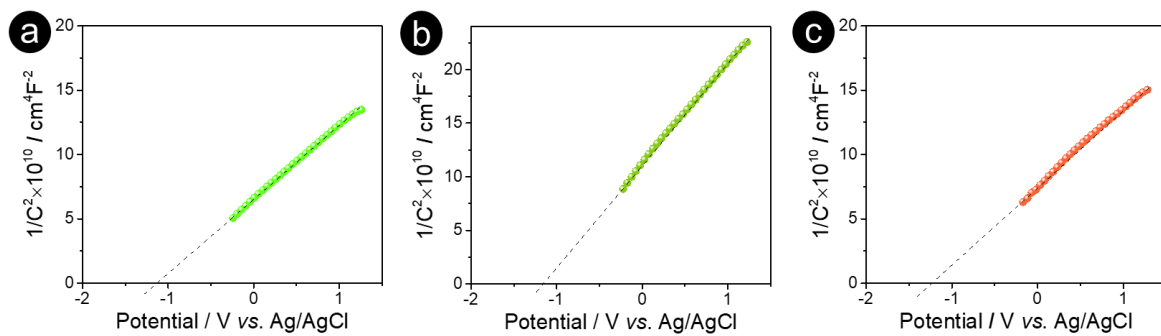


Fig. S16 Mott-Schottky plots of (a) HIAM-0001, (b) HIAM-0002 and (c) HIAM-0003.

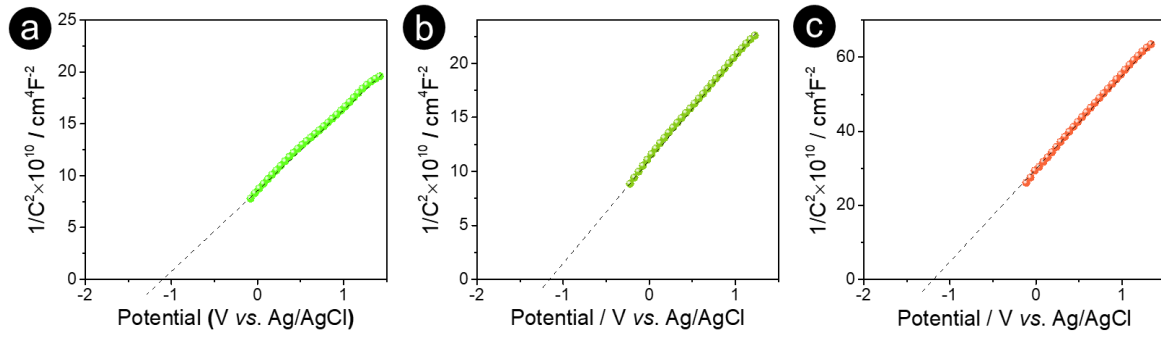


Fig. S17 Mott-Schottky plots of (a) HIAM-0004, (b) HIAM-0005 and (c) HIAM-0006.

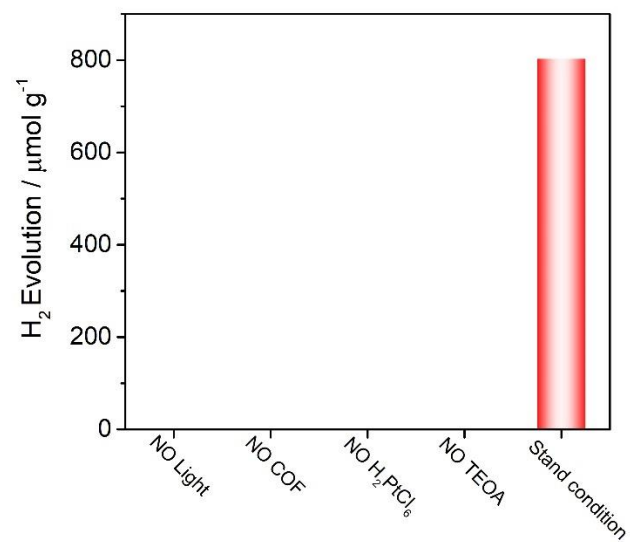


Fig. S18 The control experiments of photocatalytic H₂ evolution (Stand condition: HIAM-0001 + Light + H₂PtCl₆ + 25 vol% TEOA).

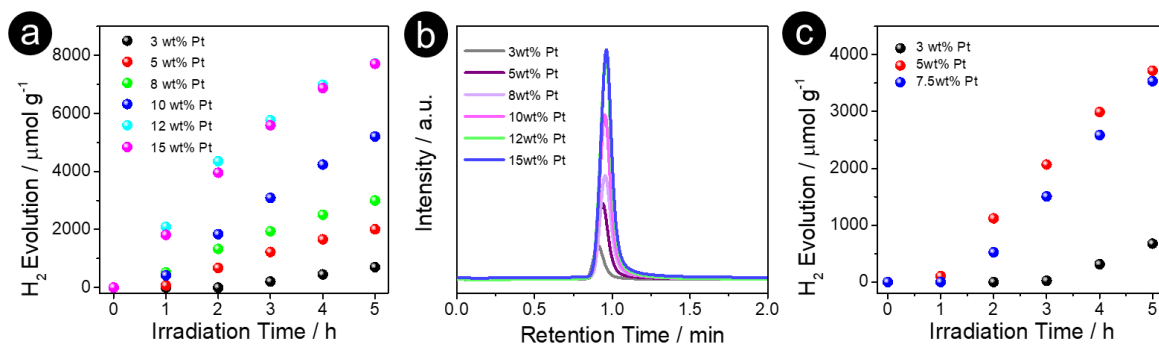


Fig. S19 The photocatalytic H₂ evolution curve of HIAM-0001 (10 mg) with different Pt contents in present of 25 vol% TEOA (50 mL H₂O) under visible-light illumination ($\lambda > 420$ nm). (b) Their corresponding GC area diagram in 25 vol% TEOA (50 mL H₂O). (c) The photocatalytic H₂ evolution curve of HIAM-0001 (10 mg) with different Pt contents in present of 0.1M AA (50 mL H₂O) under visible-light illumination ($\lambda > 420$ nm).

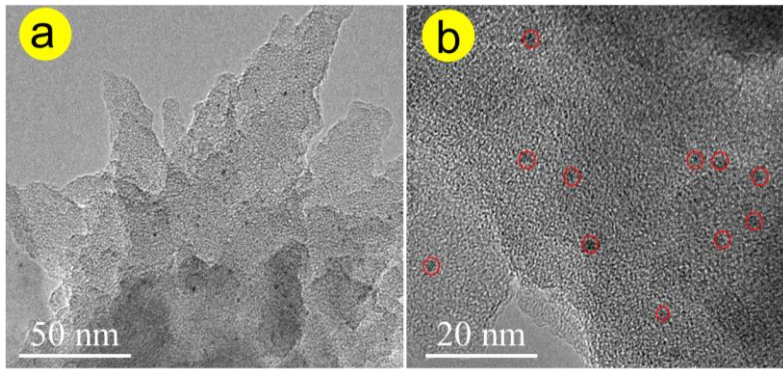


Fig. S20 TEM images of HIAM-0004 after photo-deposition of 5 wt% Pt.

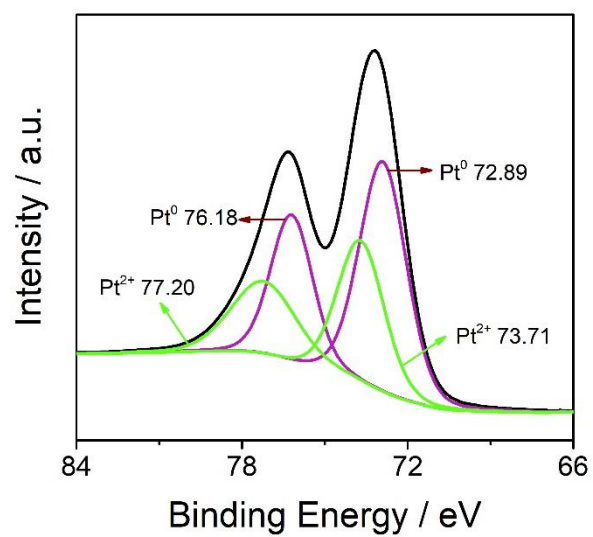


Fig. S21 Pt 4f XPS spectrum of 5 wt% Pt-loaded HIAM-0004 with AA.

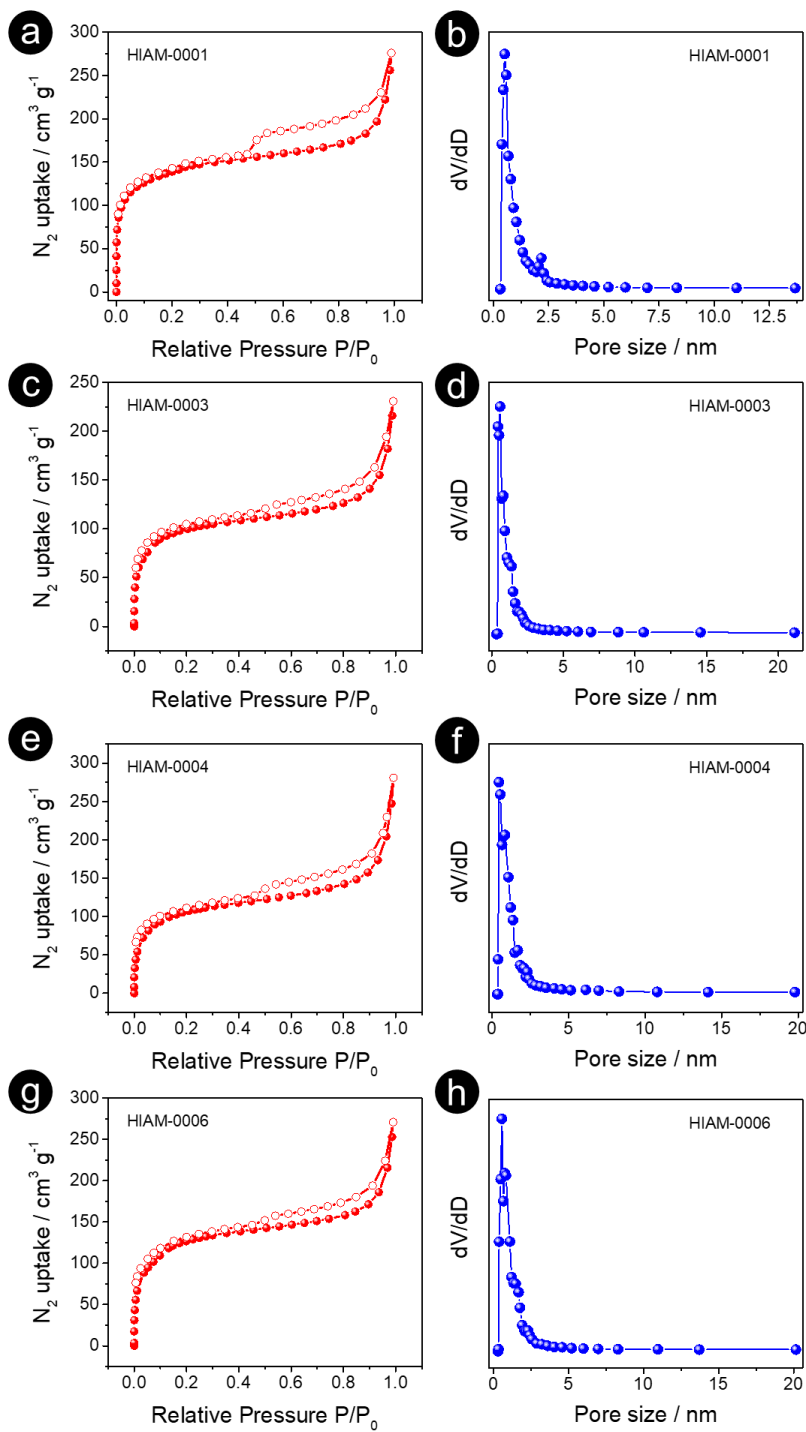


Fig. S22 Nitrogen-sorption isotherm curves of HIAM-0001 (a), HIAM-0003 (c), HIAM-0004 (e) and HIAM-0006 (g), the pore size distribution of HIAM-0001 (b), HIAM-0003 (d), HIAM-0004 (f) and HIAM-0006 (h).

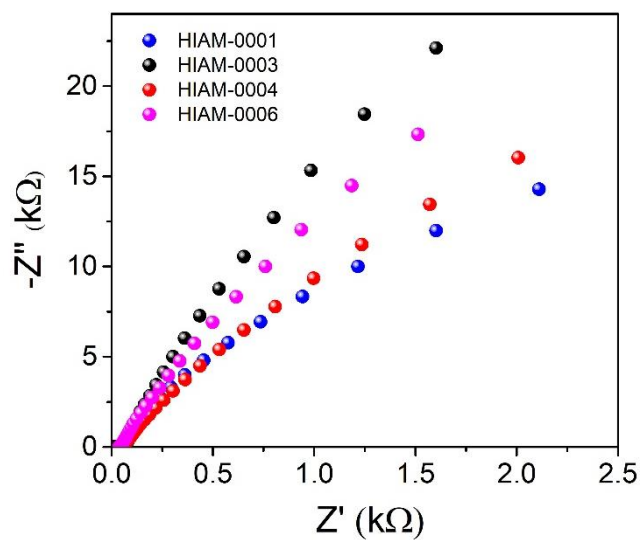


Fig. S23 Nyquist plots from electrochemical impedance spectra of HIAM-0001, HIAM-0003, HIAM-0004 and HIAM-0006 under light.

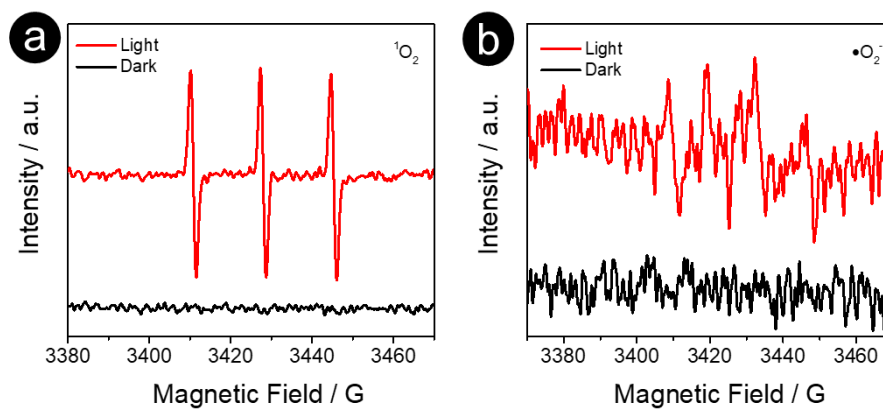


Fig. S24 EPR spectra of HIAM-0004 under dark and light irradiation.

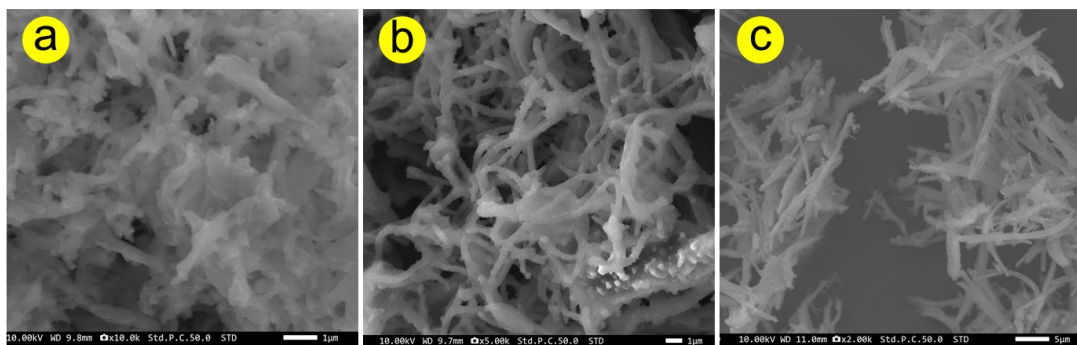


Fig. S25 SEM images of (a) HIAM-0001, (b) HIAM-0004 and (c) HIAM-0006 after photocatalytic H₂ evolution with TEOA.

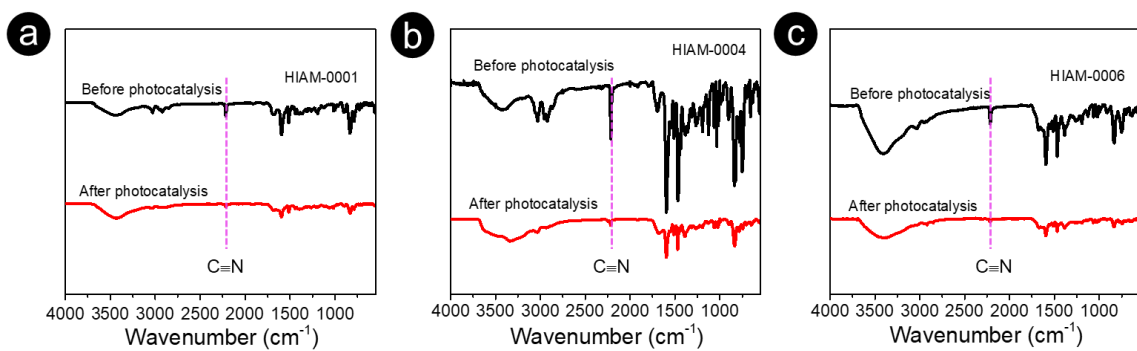


Fig. S26 FT-IR spectra of (a) HIAM-0001, (b) HIAM-0004 and (c) HIAM-0006 before and after photocatalytic H_2 evolution with TEOA.

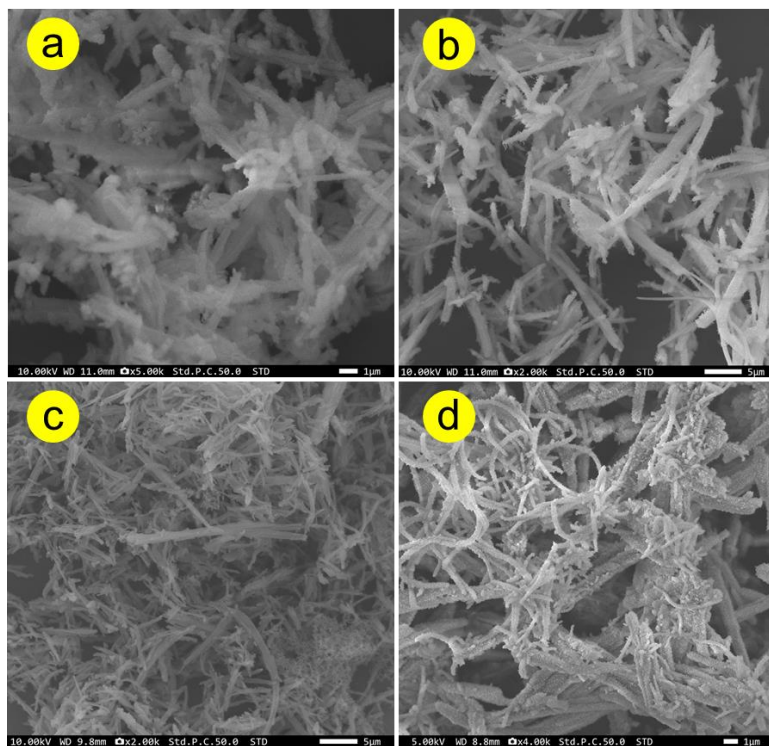


Fig. S27 SEM images of (a) HIAM-0001, (b) HIAM-0003, (c) HIAM-0004 and (d) HIAM-0006 after photocatalytic H₂ evolution with AA.

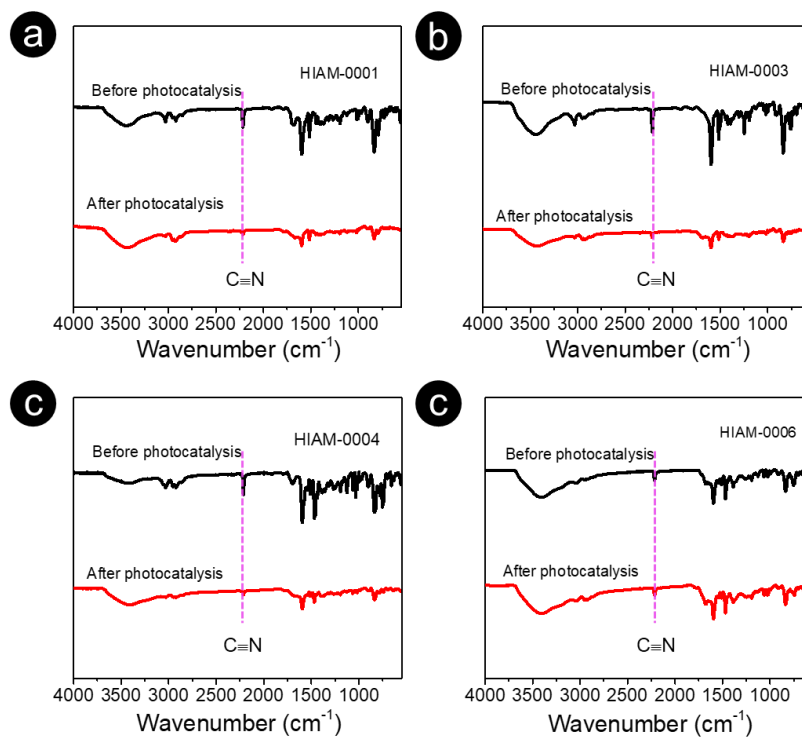


Fig. S28 FT-IR spectra of (a) HIAM-0001, (b) HIAM-0003, (c) HIAM-0004 and (d) HIAM-0006 before and after photocatalytic H₂ evolution with AA.

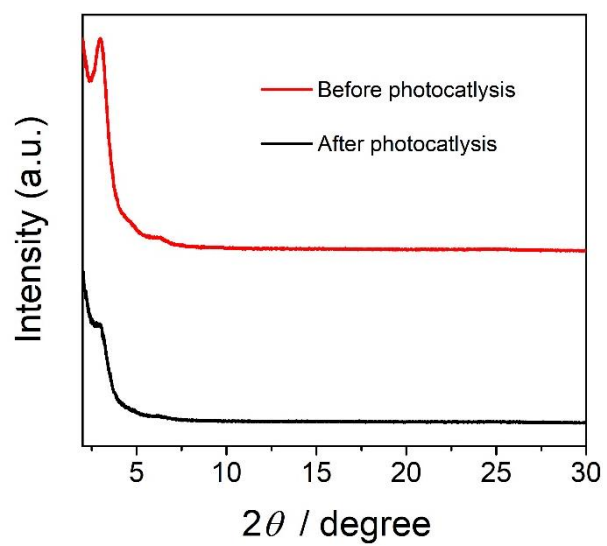


Fig. S29 PXRd patterns of HIAM-0004 before and after photocatalytic H₂ evolution.

Table S2. The HER comparison of benzothiadiazole and its derivatives-based carbon covalent organic frameworks for photocatalysis systems.

Linkage	Type	Co-catalyst	SED	HER ($\mu\text{molg}^{-1} \text{h}^{-1}$)	Ref
Imine	HPT-COF (5mg/20mL)	3wt% Pt	AA	3800	3
	BT-COF (5mg/20mL)	3wt% Pt	AA	680	3
	NKCOF-108 (10mg/100mL)	5wt% Pt	AA	12000	4
	Py-CITP-BT-COF (20mg/50mL)	5wt% Pt	AA	8875	5
	Py-FTP-BT-COF (20mg/50mL)	5wt% Pt	AA	2875	5
	Py-HTP-BT-COF (20mg/50mL)	5wt% Pt	AA	1078	5
	DPBT-TP COP (0.5mg/10mL)	7.5wt% Pt	AA	17800	6
	BT-TAPT-COF (2mg/10mL)	8wt% Pt	AA	949	7
	BTcof150 (20mg/100mL)	1wt% Pt	TEOA	750	8
	30%PEG@BT-COF (10mg/100mL)	3.5wt% Pt	AA	11140	9
Vinylene	HIAM-0001 (10mg/50mL)	5wt% Pt	AA	1410	This work
		12wt% Pt	TEOA	1217	
	HIAM-0003 (10mg/50mL)	5wt% Pt	AA	413	This work
	HIAM-0004 (10mg/50mL)	5wt% Pt	AA	1526	This work
		12wt% Pt	TEOA	1309	
	HIAM-0006 (10mg/50mL)	5wt% Pt	AA	1276	This work
		12wt% Pt	TEOA	374	

References

1. N. Zhao, C. Yang, F. Bian, D. Guo and X. Ouyang, *J. Appl. Crystallogr.*, 2022, **55**, 195-203.
2. E. Jin, K. Geng, S. Fu, M. A. Addicoat, W. Zheng, S. Xie, J.-S. Hu, X. Hou, X. Wu, Q. Jiang, Q.-H. Xu, H. I. Wang and D. Jiang, *Angew. Chem. Int. Ed.*, 2022, **61**, e202115020.
3. C. Lin, X. Liu, B. Yu, C. Han, L. Gong, C. Wang, Y. Gao, Y. Bian and J. Jiang, *ACS. Appl. Mater. Interfaces.*, 2021, **13**, 27041-27048.
4. Z. Zhao, Y. Zheng, C. Wang, S. Zhang, J. Song, Y. Li, S. Ma, P. Cheng, Z. Zhang and Y. Chen, *ACS. Catal.*, 2021, **11**, 2098-2107.
5. W. Chen, L. Wang, D. Mo, F. He, Z. Wen, X. Wu, H. Xu and L. Chen, *Angew. Chem. Int. Ed.*, 2020, **59**, 16902-16909.
6. A. M. Elewa, M. H. Elsayed, A. F. M. El-Mahdy, C.-L. Chang, L.-Y. Ting, W.-C. Lin, C.-Y. Lu and H.-H. Chou, *Appl. Catal. B Environ.*, 2021, **285**, 119802.
7. G.-B. Wang, S. Li, C.-X. Yan, Q.-Q. Lin, F.-C. Zhu, Y. Geng and Y.-B. Dong, *Chem. Commun.*, 2020, **56**, 12612-12615.
8. S. Ghosh, A. Nakada, M. A. Springer, T. Kawaguchi, K. Suzuki, H. Kaji, I. Baburin, A. Kuc, T. Heine, H. Suzuki, R. Abe and S. Seki, *J. Am. Chem. Soc.*, 2020, **142**, 9752-9762.
9. T. Zhou, L. Wang, X. Huang, J. Unruangsri, H. Zhang, R. Wang, Q. Song, Q. Yang, W. Li, C. Wang, K. Takahashi, H. Xu and J. Guo, *Nat. Commun.*, 2021, **12**, 3934.